

## Strain Control of Fermiology and Many-Body Interactions in Two-Dimensional Ruthenates

B. Burganov,<sup>1</sup> C. Adamo,<sup>2,3</sup> A. Mulder,<sup>4</sup> M. Uchida,<sup>1</sup> P. D. C. King,<sup>1,5,6</sup> J. W. Harter,<sup>1</sup> D. E. Shai,<sup>1</sup>  
A. S. Gibbs,<sup>7</sup> A. P. Mackenzie,<sup>5,8</sup> R. Uecker,<sup>9</sup> M. Bruetzam,<sup>9</sup> M. R. Beasley,<sup>3</sup> C. J. Fennie,<sup>4</sup>  
D. G. Schlom,<sup>2,6</sup> and K. M. Shen<sup>1,6,\*</sup>

<sup>1</sup>Laboratory of Atomic and Solid State Physics, Department of Physics, Cornell University, Ithaca, New York 14853, USA

<sup>2</sup>Department of Materials Science and Engineering, Cornell University, Ithaca, New York 14853, USA

<sup>3</sup>Department of Applied Physics, Stanford University, Stanford, California 94305, USA

<sup>4</sup>School of Applied and Engineering Physics, Cornell University, Ithaca, New York 14853, USA

<sup>5</sup>School of Physics and Astronomy, University of St Andrews, St Andrews, Fife KY16 9SS, United Kingdom

<sup>6</sup>Kavli Institute at Cornell for Nanoscale Science, Ithaca, New York 14853, USA

<sup>7</sup>Max Planck Institute for Solid State Research, 70569 Stuttgart, Germany

<sup>8</sup>Max Planck Institute for Chemical Physics of Solids, D-01187 Dresden, Germany

<sup>9</sup>Leibniz Institute for Crystal Growth, D-12489 Berlin, Germany

(Received 20 January 2016; published 13 May 2016)

Here we demonstrate how the Fermi surface topology and quantum many-body interactions can be manipulated via epitaxial strain in the spin-triplet superconductor  $\text{Sr}_2\text{RuO}_4$  and its isoelectronic counterpart  $\text{Ba}_2\text{RuO}_4$  using oxide molecular beam epitaxy, *in situ* angle-resolved photoemission spectroscopy, and transport measurements. Near the topological transition of the  $\gamma$  Fermi surface sheet, we observe clear signatures of critical fluctuations, while the quasiparticle mass enhancement is found to increase rapidly and monotonically with increasing Ru-O bond distance. Our work demonstrates the possibilities for using epitaxial strain as a disorder-free means of manipulating emergent properties, many-body interactions, and potentially the superconductivity in correlated materials.

DOI: 10.1103/PhysRevLett.116.197003

Pressure plays a key role in modifying the properties of materials with strong electronic correlations, for instance, enhancing the transition temperature of the cuprate superconductors or driving quantum phase transitions in heavy fermion systems. Unfortunately, leading techniques for investigating the electronic structure, such as angle-resolved photoemission spectroscopy (ARPES) and STM, are incompatible with typical high pressure or strain apparatus. The epitaxial growth of thin films on deliberately lattice mismatched substrates provides a clean and accessible analogue to external pressure and has been used to dramatically alter the electronic phases of many complex oxides [1–4]. In the family of ruthenium oxides, the strong structure-property relationship leads to a wide variety of ground states including unconventional superconductivity [5], metamagnetism and electronic liquid crystalline states [6–8], ferromagnetism, antiferromagnetism and spin-glass behavior [9–11], without changing the formal oxidation state of the Ru ion. Among them,  $\text{Sr}_2\text{RuO}_4$  is an ideal candidate to explore the effects of biaxial strain and chemical pressure, since the extreme sensitivity of its superconducting ground state to disorder [12] precludes enhancement of  $T_c$  through chemical substitution. The possibly chiral nature of the superconducting state has given rise to proposals utilizing  $\text{Sr}_2\text{RuO}_4$  as a platform for realizing Majorana fermions, exotic Josephson junctions,

and non-Abelian topological quantum computation [13,14]. Hydrostatic pressure was shown to suppress both the  $T_c$  [15] and quasiparticle enhancements [16], but recent experiments applying a uniaxial strain of 0.2% demonstrated a strong nonlinear enhancement of  $T_c$  [17]. Obtaining uniaxial strains of greater than 0.5% is a challenge in rather brittle metal oxides, but biaxial strains of 2%–3% are readily achievable in epitaxial thin films grown on deliberately lattice mismatched substrates. Here we demonstrate epitaxial strain engineering as a disorder-free means to dramatically manipulate the electronic structure of  $\text{Sr}_2\text{RuO}_4$  and its sister compound,  $\text{Ba}_2\text{RuO}_4$ , through a combination of reactive oxide molecular beam epitaxy (MBE) growth and *in situ* ARPES. We are able to observe a topological transition in the  $\gamma$  Fermi surface (FS) sheet (i.e., a Lifshitz transition) through the selection of appropriate substrates. In addition, we observe signatures of quantum criticality in both ARPES and electrical transport near the Lifshitz transition, as well as a surprisingly large enhancement of the quantum many-body interactions with increasing in-plane lattice constant.

Thin films of  $\text{Sr}_2\text{RuO}_4$  and  $\text{Ba}_2\text{RuO}_4$  were synthesized by reactive oxide MBE and the in-plane lattice constant (i.e., the Ru-O-Ru bond distance) can be increased from 3.87 to 3.97 Å ( $\Delta a/a = 2.6\%$ ) through the selection of appropriate substrates.  $\text{Sr}_2\text{RuO}_4$  films were found to relax

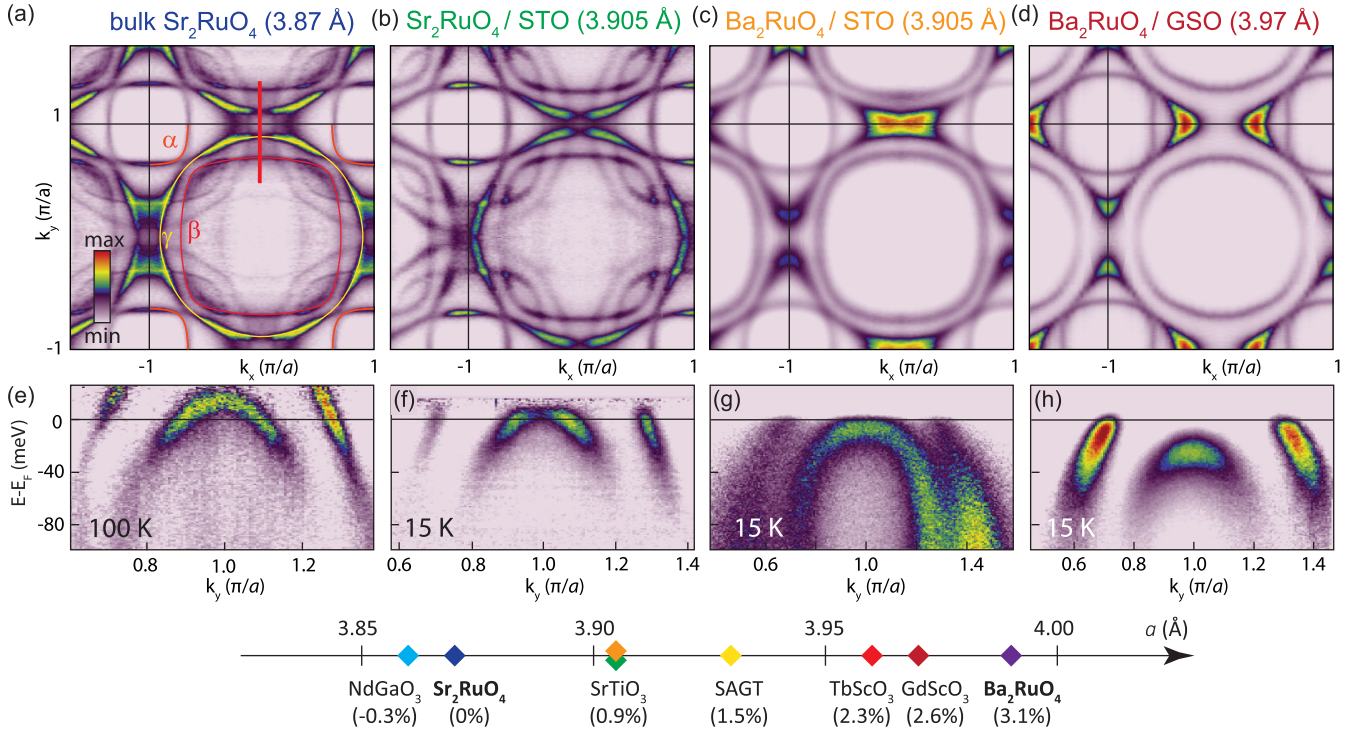


FIG. 1. (a)–(d) Fermi surface maps and (e)–(h) spectral weight along the  $(0, k_y)$  direction [thick red line in (a)] for select strain states of  $\text{Sr}_2\text{RuO}_4$  and  $\text{Ba}_2\text{RuO}_4$ . The data in (e) were measured at an elevated temperature ( $T = 100$  K) to thermally populate the states above the Fermi level; the rest of the data in the Letter were taken at 15 K. To show the dispersion near the vHs above  $E_F$ , the spectral weight was divided by the Fermi function in (e) and (f). The substrate number line shows the room temperature lattice constants and strain values relative to bulk  $\text{Sr}_2\text{RuO}_4$ .

immediately at lattice constants larger than  $3.91 \text{ \AA}$ , thus necessitating the substitution of Ba for Sr as the A-site cation to achieve even larger in-plane lattice constants. In bulk,  $\text{Ba}_2\text{RuO}_4$  crystallizes in a hexagonal polymorph, and the  $\text{K}_2\text{NiF}_4$  structure is metastable and has only been synthesized in polycrystalline form above 6 GPa [18]. Epitaxial stabilization has, however, been employed to realize thin films of tetragonal  $\text{Ba}_2\text{RuO}_4$  [19] which we show are isostructural and isoelectronic to  $\text{Sr}_2\text{RuO}_4$ .

The electronic structure of bulk  $\text{Sr}_2\text{RuO}_4$  is highly two-dimensional and comprised of four electrons in the Ru  $4d$   $t_{2g}$  orbitals, which form the quasi-1D  $\alpha$  and  $\beta$  FS sheets (primarily of  $d_{xz}$  and  $d_{yz}$  character), and the quasi-2D  $\gamma$  sheet (primarily  $d_{xy}$ ). In Figure 1, we show a series of ARPES FS maps as a function of increasing in-plane lattice constant on a bulk single crystal of  $\text{Sr}_2\text{RuO}_4$  cleaved at elevated temperature ( $a = 3.869 \text{ \AA}$ ),  $\text{Sr}_2\text{RuO}_4$  grown on  $\text{SrTiO}_3$  (STO;  $a = 3.905 \text{ \AA}$ ),  $\text{Ba}_2\text{RuO}_4$  grown on  $\text{SrTiO}_3$  ( $a = 3.905 \text{ \AA}$ ), and  $\text{Ba}_2\text{RuO}_4$  grown on  $\text{GdScO}_3$  (GSO;  $a = 3.968 \text{ \AA}$ ). The data from the single crystal of  $\text{Sr}_2\text{RuO}_4$  [Fig. 1(a)] show all three bulk FS sheets, as well as a  $\sqrt{2} \times \sqrt{2}$  surface reconstruction, which generates additional sets of folded surface-derived bands [20,21]. The  $\sqrt{2} \times \sqrt{2}$  surface reconstruction is still apparent in Fig. 1(b), indicating that the reconstruction is also present on the

natively grown surface. One of the unique hallmarks of  $\text{Sr}_2\text{RuO}_4$  is the presence of a saddle point at  $(\pi, 0)$  and  $(0, \pi)$ , which gives rise to a van Hove singularity (vHs) only 14 meV above the Fermi energy [ $E_F$ , Fig. 1(e)]. When this vHs passes through  $E_F$ , the  $\gamma$  sheet undergoes a topological transition from electronlike to holelike. For the thin film of  $\text{Sr}_2\text{RuO}_4/\text{STO}$  [Fig. 1(b)], the  $\gamma$  FS sheet is noticeably enlarged versus bulk and the vHs is pushed down to 9 meV above  $E_F$ .

For  $\text{Ba}_2\text{RuO}_4$  on  $\text{SrTiO}_3$  [Fig. 1(c)], the  $\gamma$  FS is almost precisely at the topological transition between electron and holelike, and the vHs is nearly at  $E_F$  [4 meV below, Fig. 1(g)]. Although the samples shown in Fig. 1(b) and 1(c) are both grown on  $\text{SrTiO}_3$ ,  $\text{Ba}_2\text{RuO}_4/\text{SrTiO}_3$  is much closer to the topological transition primarily due to the reduced second nearest neighbor hopping ( $t_4/t_1$ ) which changes the shape of the  $\gamma$  FS and lowers the vHs [22]. For  $\text{Ba}_2\text{RuO}_4$  grown on  $\text{GdScO}_3$ , the vHs is now well below  $E_F$  [25 meV below, Fig. 1(h)], and the  $\gamma$  FS clearly forms a holelike sheet centered around  $(\pi, \pi)$ . The surface reconstruction is absent in  $\text{Ba}_2\text{RuO}_4$  films, likely due to the larger Ba cation radius ( $\text{Ba}^{2+}$ :  $1.47 \text{ \AA}$  vs  $\text{Sr}^{2+}$ :  $1.31 \text{ \AA}$  [31]) which should impede the freezing of the  $\Sigma_3$  phonon mode on the surface. It is also notable that the  $\beta$  FS sheet becomes noticeably less 1D, due to the increased transverse hopping between  $d_{xz/yz}$  orbitals ( $t_3/t_2$ ).

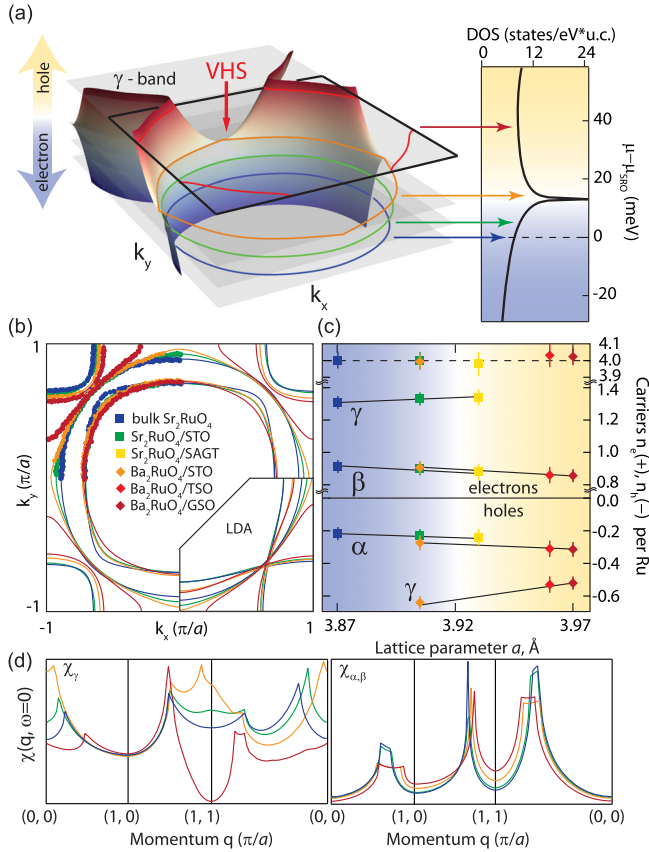


FIG. 2. (a) Schematic showing the evolution of the  $\gamma$  Fermi surface and density of states at  $E_F$  as a result of strain and negative chemical pressure by  $A$ -site substitution. (b) Tight-binding parametrization of ARPES Fermi surfaces and LDA Fermi surfaces. (c) Luttinger volume of experimental Fermi pockets as a function of the in-plane lattice parameter. The total number of electrons adds up to  $n = 4.00 \pm 0.05$  showing negligible overall doping. (d) Lindhard susceptibility calculated for the two-dimensional  $\gamma$  and one-dimensional  $\alpha/\beta$  pockets from the experimental Fermi surfaces.

A schematic of the strain evolution of the  $\gamma$  FS is shown in Fig. 2(a), where the vertical axis is the effective change in the chemical potential of the  $\gamma$ -band relative to bulk  $\text{Sr}_2\text{RuO}_4$ . The change in FS topology cannot be described simply as a rigid shift of the bulk bands; the Fermi surfaces and density of states shown in Figs. 2(a) and 2(b) are generated from a generalized tight binding model whose parameters are varied to fit the different strained samples [22]. The filling of the  $\gamma$  band arises from interorbital electron transfer from the  $d_{xz}$  and  $d_{yz}$  orbitals into the  $d_{xy}$  orbital; the total number of electrons in all three bands remains constant at  $4.00 \pm 0.05$  [Fig. 2(c)]. Although density functional calculations indicate that the spin-orbit interaction is non-negligible [32], we could not directly resolve any spin-orbit split bands, possibly due to impurity scattering and/or experimental resolution. Therefore, we simply utilize a typical 3-band tight-binding model to parametrize our data. The Lifshitz transition has a profound impact on the electron-hole susceptibility, as shown by the

Lindhard susceptibility for the 2D  $\gamma$  band and the 1D  $\alpha$  and  $\beta$  bands calculated using a tight-binding parametrization of the experimental FS wave vectors and dispersion. Only intraband scattering for  $\gamma$  is considered, while both intra- and interband scattering between the 1D  $\alpha$  and  $\beta$  bands is allowed. For the 1D bands,  $\chi_{\alpha,\beta}(\mathbf{q}, \omega = 0)$  is relatively independent of strain, except for the reduced nesting in  $\text{Ba}_2\text{RuO}_4$  due to its stronger two-dimensionality. For the  $\gamma$  band, however,  $\chi_\gamma(\mathbf{q}, \omega = 0)$  exhibits dramatic changes with strain, where  $\chi_\gamma(\mathbf{q} = (0, 0))$  is strongly enhanced approaching the Lifshitz transition. There is also a corresponding increase of  $\chi_\gamma(\mathbf{q} = (\pm\pi, \pm\pi))$ , since that wave vector connects the vHs at  $(0, \pi)$  and  $(\pi, 0)$  to symmetry-equivalent pairs. This detailed parametrization of the electronic structure and susceptibility at different strain states should provide valuable input to make falsifiable predictions for the behavior of the superconducting state with strain, as well as help to distinguish which bands are most relevant to superconductivity [33–35].

The impact of the topological transition is clearly evident in the electrical resistivity and in spectroscopic signatures. Between  $T_c$  and 25 K, bulk  $\text{Sr}_2\text{RuO}_4$  behaves as an ideal Fermi liquid with a  $T^2$  resistivity and moderate correlations [36,37]. This  $T^2$  resistivity is also observed for  $\text{Sr}_2\text{RuO}_4$  and  $\text{Ba}_2\text{RuO}_4$  films on either side of the Lifshitz transition

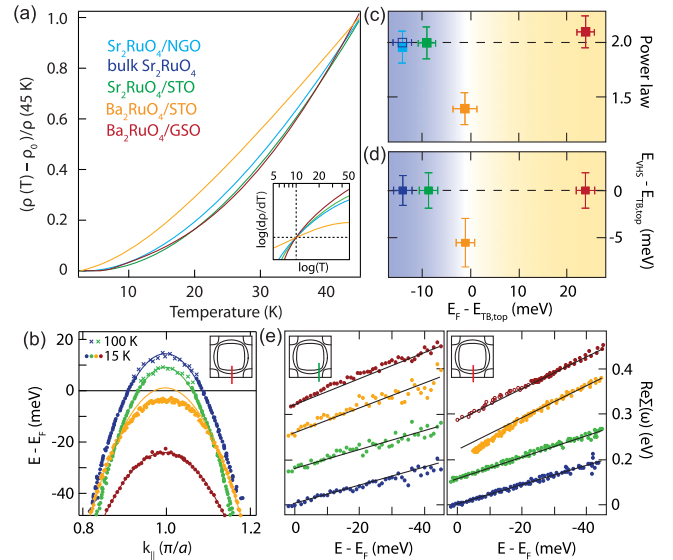


FIG. 3. Normalized resistivity fitted to  $\rho \propto T^n$  [values of  $n$  shown in (c) with the open symbol from Ref. [36]]. The inset shows  $\log(dp/dT) \approx (n-1)\log(T)$  with an offset. (b) Dispersion of the  $\gamma$  band along  $(0,0) - (0,\pi)$ , and (d) the deviation of  $E_{\text{VHS}}$  from the TB model. (e)  $\text{Re}\Sigma(\omega)$  (offset at  $E = E_F$  is included for clarity).  $\text{Re}\Sigma(\omega) \propto \omega$  implies quadratic energy dependence of the quasiparticle scattering rate  $\Gamma(\omega) \propto \text{Im}\Sigma(\omega) \propto \omega^2$  expected for a Fermi liquid.  $\text{Ba}_2\text{RuO}_4/\text{STO}$  acquires additional kinklike features in the real part at the energy scale of  $15 \pm 10$  meV near  $\mathbf{k} = (0, \pi)$  (red line cut). This flattens the  $\gamma$  band and pushes the vHs slightly below the Fermi level.

(Fig. 3(a)). Close to the Lifshitz transition, however, we observe  $\rho(T) \propto T^{1.4 \pm 0.1}$  up to approximately 25 K in  $\text{Ba}_2\text{RuO}_4/\text{STO}$  as shown in Figs. 3(a) and 3(c), consistent with a previous doping-dependent study [38]. The quasiparticle dispersion at  $(\pi, 0)$  also exhibits a deviation from the calculated band structure precisely at the vHs for  $\text{Ba}_2\text{RuO}_4/\text{STO}$ , as shown in Fig. 3(b). At other strain states, the experimental dispersion at  $(\pi, 0)$  can be well described by a tight binding fit. At the critical strain state, however, the dispersion exhibits an anomalous flattening which deviates strongly from both the LDA calculations and the tight binding parametrization, and cannot be ascribed to the finite experimental resolution [22]. This can be represented by a deviation of  $\Sigma'(w)$  at  $\mathbf{k} = (\pi, 0)$  from a linear dependence at low energy expected for a conventional Fermi liquid and observed at other locations in momentum space for  $\text{Ba}_2\text{RuO}_4/\text{STO}$  [Fig. 3(e)]. Since the low-energy electronic structure is highly two-dimensional, the measured quasiparticle properties in  $\text{Ba}_2\text{RuO}_4/\text{STO}$  appear to be unaffected by any finite thickness effects [22]. The thin films presented here are nonsuperconducting, with residual resistivities  $\rho_0 \approx 10^{-5} \Omega \text{ cm}$ , although recent upgrades to the growth chamber should allow us to ultimately achieve superconducting films, as has been reported in unstrained thin films grown on LSAT [39].

Given the deviations from canonical Fermi liquid behavior, it is natural to investigate whether the strength of quantum many-body interactions is likewise peaked at the Lifshitz transition. This is shown in Fig. 4, where the measured quasiparticle dispersions  $E(k)$  for the  $\alpha$  and  $\beta$  bands are shown as a function of in-plane lattice constant. Figures 4(g)–4(i) summarize the quasiparticle mass renormalization for all three bands crossing  $E_F$ . The mass enhancements were calculated using the dispersion along the line cuts for the  $\alpha$  and  $\beta$  bands and averaged over the full BZ for the  $\gamma$  band [22]. It has been established from both quantum oscillations and prior ARPES measurements that the mass renormalization of  $\alpha$  and  $\beta$  bands in bulk  $\text{Sr}_2\text{RuO}_4$  is approximately 2.5–3 [40,41], consistent with our measurements on single crystals of  $\text{Sr}_2\text{RuO}_4$ . The strength of this renormalization is, however, dramatically enhanced when increasing the Ru-O bond length and substituting the larger A-site cation. Increasing the bond distance by 2.6% when going from bulk  $\text{Sr}_2\text{RuO}_4$  to  $\text{Ba}_2\text{RuO}_4$  on GSO, increases the effective mass of the  $\alpha$  band by nearly a factor of 2, far larger than expected than from LDA, which predict less than a 10% change in  $v_F$  between these two materials [Fig. 4(g)], yet a noticeable jump in the renormalization occurs when changing from the Sr to Ba cation at the same lattice constant ( $\text{SrTiO}_3$ ). In the  $\alpha$  and  $\beta$  bands, a significant component of the mass enhancement arises from a kink in the dispersion (presumably due to electron-boson coupling) around  $80 \pm 40 \text{ meV}$ . Nevertheless, even the dispersion at higher binding energies (greater than 100 meV) is substantially renormalized in going from bulk  $\text{Sr}_2\text{RuO}_4$  to

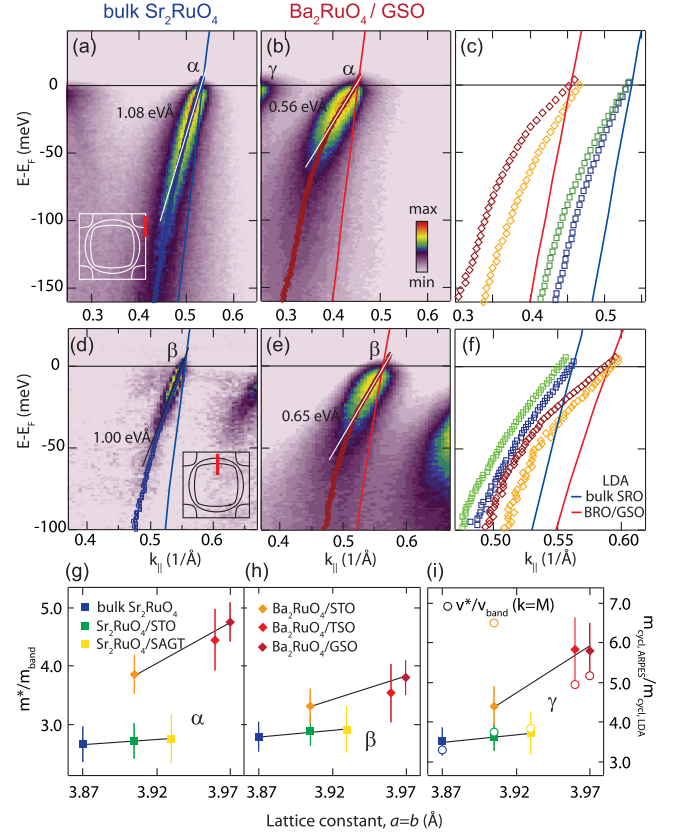


FIG. 4. Dispersion  $E(k)$  of the  $\alpha$  band along the BZ boundary (a)–(c) and  $\beta$  band along  $(0,0)$ – $(0, \pi)$  (d)–(f). Spectral weight is shown for the single crystal  $\text{Sr}_2\text{RuO}_4$  (a),(d) and  $\text{Ba}_2\text{RuO}_4/\text{GSO}$  (b),(e). The colors of the open symbols in (c) and (f) are consistent with the colors in (g)–(i). Quasiparticle renormalizations for the  $\alpha$  band (g) and  $\beta$  band (h) have strong monotonic dependence on the strain value. QP renormalization for the  $\gamma$  band (i), calculated as a ratio of the LDA bandwidth to ARPES bandwidth from the corresponding tight-binding fits, shows a similar monotonic increase as a function of tensile strain. The open circles in (i) show the band renormalization from the slope of the real part of self-energy  $1 - \partial \text{Re}\Sigma(\omega)/\partial \omega$  near  $E_F$  calculated at  $\mathbf{k} = (\pi, 0)$ . The deviation for  $\text{Ba}_2\text{RuO}_4/\text{STO}$  is due to the band flattening shown in Fig. 3(b).

$\text{Ba}_2\text{RuO}_4/\text{GSO}$  (a factor of  $1.9 \pm 0.2$  and  $1.8 \pm 0.4$  for the  $\alpha$  and  $\beta$  bands, respectively). It is important to note that the mass enhancement is not peaked at the Lifshitz transition, but rather increases monotonically with Ru-O bond distance, consistent with the increase of correlations from the local repulsion  $U/t$  and the Hund's coupling [42,43].

At this point, we compare strain-induced modifications to prior carrier doping studies [41]. One advantage of strain is the potential to investigate its impact on superconductivity and  $T_c$ , whereas chemical disorder destroys superconductivity. Like in doped  $\text{Sr}_{2-y}\text{La}_y\text{RuO}_4$ , we observe signatures of criticality (e.g.,  $\rho \propto T^{1.4}$  behavior) at low temperatures near the Lifshitz transition [38]. Some effects of criticality might be partially masked by disorder, which can be improved in future generations of thin films. The

impact of electron doping on the electronic structure of  $\text{Sr}_{2-y}\text{La}_y\text{RuO}_4$  could be well described by a simple rigid band shift model, and there was no change in the mass renormalization, even past the Lifshitz transition. In contrast, epitaxial strain impacts the electronic structure in more profound ways, including inducing large increases in the mass renormalization (Fig. 4), and an unexpected band flattening near the Lifshitz transition [Figs. 3(b) and 3(d)]. The strength of the low-energy kink around 80 meV in the  $\alpha$  and  $\beta$  bands are also greatly enhanced in  $\text{Ba}_2\text{RuO}_4$  versus  $\text{Sr}_2\text{RuO}_4$ , suggesting an increased electron-phonon interaction, which was not reported in  $\text{Sr}_{2-y}\text{La}_y\text{RuO}_4$ . In comparison to the prior work on uniaxial strain [17], our calculations indicate that the impact to the electronic structure along the strained direction is comparable to the effects of biaxial strain. However, under uniaxial strain  $C_4$  symmetry is broken, and therefore one pair of van Hove singularities is lowered, while the orthogonal pair is raised in energy. Nevertheless, the uniaxial strain experiments suggest that superconductivity may be strongly intertwined with lowering the vHs, and therefore we speculate that biaxial strain could likewise be a promising route towards enhancing  $T_c$ , as will be addressed by a future theoretical study [44].

Our work is the first demonstration of controlling Fermi surface topology and quantum many-body interactions in ruthenates via epitaxial strain engineering, opening the door to future possibilities for engineering quantum many-body ground states in a disorder-free manner to explore enhanced superconductivity, quantum criticality, or electronic nematic states. Tuning the  $\gamma$  FS sheet precisely to the Lifshitz transition allows us to place the system at the onset of quantum criticality and observe deviations from canonical Fermi liquid behavior. Our work demonstrates strong interorbital electron transfer between the different  $t_{2g}$  orbitals with increasing strain, and a topological transition in the  $\gamma$  FS sheet. The detailed parametrization of the evolution of the fermiology and mass renormalization should allow for testable theoretical predictions for changes in the superconducting state with epitaxial strain.

We thank A. Georges, Y. T. Hsu, and E. A. Kim for helpful discussions and suggestions. This work was primarily supported by Air Force Office of Scientific Research (Grants No. FA9550-12-1-0335 and No. FA2386-12-1-3013). Support from the National Science Foundation was through the Materials Research Science and Engineering Centers program (DMR-1120296, the Cornell Center for Materials Research). This work was performed in part at the Cornell NanoScale Facility, a member of the National Nanotechnology Infrastructure Network, which is supported by the National Science Foundation (Grant No. ECCS-0335765). M. U. acknowledges support from a Postdoctoral Fellowship for Research Abroad (No. 24-162) from the Japanese Society for the Promotion of Science.

B. B. and C. A. contributed equally to this work.

\*To whom correspondence should be addressed.

kmsheh@cornell.edu

- [1] J. P. Locquet, J. Perret, J. Fompeyrine, E. Machler, J. W. Seo, and G. Van Tendeloo, *Nature (London)* **394**, 453 (1998).
- [2] K. J. Choi, M. Biegalski, Y. L. Li, A. Sharan, J. Schubert, R. Uecker, P. Reiche, Y. B. Chen, X. Q. Pan, V. Gopalan, L.-Q. Chen, and D. G. Schlom, and C. B. Eom, *Science* **306**, 1005 (2004).
- [3] J. H. Lee, L. Fang, E. Vlahos, X. Ke, Y. W. Jung, L. F. Kourkoutis, J.-W. Kim, P. J. Ryan, T. Heeg, M. Roeckerath, V. Goian, M. Bernhagen, R. Uecker, P. C. Hammel, K. M. Rabe, S. Kamba, J. Schubert, J. W. Freeland, D. A. Muller, C. J. Fennie, P. Schiffer, V. Gopalan, E. Johnston-Halperin, and D. G. Schlom, *Nature (London)* **466**, 954 (2010).
- [4] H. K. Yoo, S. I. Hyun, L. Moreschini, H.-D. Kim, Y. J. Chang, C. H. Sohn, D. W. Jeong, S. Sinn, Y. S. Kim, A. Bostwick, E. Rotenberg, J. H. Shim, and T. W. Noh, *Sci. Rep.* **5**, 8746 (2015).
- [5] Y. Maeno, H. Hashimoto, K. Yoshida, S. Nishizaki, T. Fujita, J. G. Bednorz, and F. Lichtenberg, *Nature (London)* **372**, 532 (1994).
- [6] S. A. Grigera, R. S. Perry, A. J. Schofield, M. Chiao, S. R. Julian, G. G. Lonzarich, S. I. Ikeda, Y. Maeno, A. J. Millis, and A. P. Mackenzie, *Science* **294**, 329 (2001).
- [7] R. A. Borzi, S. A. Grigera, J. Farrell, R. S. Perry, S. J. S. Lister, S. L. Lee, D. A. Tennant, Y. Maeno, and A. P. Mackenzie, *Science* **315**, 214 (2007).
- [8] C. Lester, S. Ramos, R. S. Perry, T. P. Croft, R. I. Bewley, T. Guidi, P. Manuel, D. D. Khalyavin, E. Forgan, and S. M. Hayden, *Nat. Mater.* **14**, 373 (2015).
- [9] J. M. Longo, P. M. Raccach, and J. B. Goodenough, *J. Appl. Phys.* **39**, 1327 (1968).
- [10] S. Nakatsuji and Y. Maeno, *Phys. Rev. Lett.* **84**, 2666 (2000).
- [11] J. P. Carlo, T. Goko, I. M. Gat-Malureanu, P. L. Russo, A. T. Savici, A. A. Aczel, G. J. MacDougall, J. A. Rodriguez, T. J. Williams, G. M. Luke, C. R. Wiebe, Y. Yoshida, S. Nakatsuji, Y. Maeno, T. Taniguchi, and Y. J. Uemura, *Nat. Mater.* **11**, 323 (2012).
- [12] A. P. Mackenzie, R. K. W. Haselwimmer, A. W. Tyler, G. G. Lonzarich, Y. Mori, S. Nishizaki, and Y. Maeno, *Phys. Rev. Lett.* **80**, 161 (1998).
- [13] Y. Ueno, A. Yamakage, Y. Tanaka, and M. Sato, *Phys. Rev. Lett.* **111**, 087002 (2013).
- [14] P. M. R. Brydon, C. Iniotakis, D. Manske, and M. Sigrist, *Phys. Rev. Lett.* **104**, 197001 (2010).
- [15] N. Shirakawa, K. Murata, S. Nishizaki, Y. Maeno, and T. Fujita, *Phys. Rev. B* **56**, 7890 (1997).
- [16] D. Forsythe, S. R. Julian, C. Bergemann, E. Pugh, M. J. Steiner, P. L. Alireza, G. J. McMullan, F. Nakamura, R. K. W. Haselwimmer, I. R. Walker, S. S. Saxena, G. G. Lonzarich, A. P. Mackenzie, Z. Q. Mao, and Y. Maeno, *Phys. Rev. Lett.* **89**, 166402 (2002).
- [17] C. W. Hicks, D. O. Brodsky, E. A. Yelland, A. S. Gibbs, J. A. N. Bruin, M. E. Barber, S. D. Edkins, K. Nishimura, S. Yonezawa, Y. Maeno, and A. P. Mackenzie, *Science* **344**, 283 (2014).
- [18] J. Kafalas and J. Longo, *J. Solid State Chem.* **4**, 55 (1972).
- [19] Y. Jia, M. A. Zurbuchen, S. Wozniak, A. H. Carim, D. G. Schlom, L.-N. Zou, S. Briczinski, and Y. Liu, *Appl. Phys. Lett.* **74**, 3830 (1999).

- [20] R. Matzdorf, Z. Fang, Ismail, J. Zhang, T. Kimura, Y. Tokura, K. Terakura, and E. W. Plummer, *Science* **289**, 746 (2000).
- [21] A. Damascelli, D. H. Lu, K. M. Shen, N. P. Armitage, F. Ronning, D. L. Feng, C. Kim, Z. X. Shen, T. Kimura, Y. Tokura, Z. Q. Mao, and Y. Maeno, *Phys. Rev. Lett.* **85**, 5194 (2000).
- [22] See Supplemental Material <http://link.aps.org/supplemental/10.1103/PhysRevLett.116.197003> for the details of sample growth, characterization, *ab initio* calculations and tight-binding model, which includes Refs. [23–30].
- [23] L. Waltz and F. Lichtenberg, *Acta Crystallogr. Sect. C* **49**, 1268 (1993).
- [24] R. Uecker, D. Klimm, R. Bertram, M. Bernhagen, I. Schulze-Jonack, M. Bruetzsch, A. Kwasniewski, Th. M. Gesing, and D. G. Schlom, *Acta Phys. Pol. A* **124**, 295 (2013).
- [25] D. G. Schlom, L.-Q. Chen, C. J. Fennie, V. Gopalan, D. A. Muller, X. Pan, R. Ramesh, and R. Uecker, *MRS Bull.* **39**, 118 (2014).
- [26] K. M. Shen, A. Damascelli, D. H. Lu, N. P. Armitage, F. Ronning, D. L. Feng, C. Kim, Z.-X. Shen, D. J. Singh, I. I. Mazin, S. Nakatsuji, Z. Q. Mao, Y. Maeno, T. Kimura, and Y. Tokura, *Phys. Rev. B* **64**, 180502 (2001).
- [27] E. P. Abrahams, P. W. Anderson, P. A. Lee, and T. V. Ramakrishnan, *Phys. Rev. B* **24**, 6783 (1981).
- [28] C. N. Veenstra, Z.-H. Zhu, B. Ludbrook, M. Capsoni, G. Levy, A. Nicolaou, J. A. Rosen, R. Comin, S. Kittaka, Y. Maeno, I. S. Elfimov, and A. Damascelli, *Phys. Rev. Lett.* **110**, 097004 (2013).
- [29] P. E. Blöchl, *Phys. Rev. B* **50**, 17953 (1994).
- [30] G. Kresse and J. Furthmüller, *Phys. Rev. B* **54**, 11169 (1996).
- [31] R. D. Shannon, *Acta Cryst.* **A32**, 751 (1976).
- [32] M. W. Haverkort, I. S. Elfimov, L. H. Tjeng, G. A. Sawatzky, and A. Damascelli, *Phys. Rev. Lett.* **101**, 026406 (2008).
- [33] S. Raghu, A. Kapitulnik, and S. A. Kivelson, *Phys. Rev. Lett.* **105**, 136401 (2010).
- [34] J.-W. Huo, T. M. Rice, and F.-C. Zhang, *Phys. Rev. Lett.* **110**, 167003 (2013).
- [35] I. I. Mazin and D. J. Singh, *Phys. Rev. Lett.* **79**, 733 (1997).
- [36] N. E. Hussey, A. P. Mackenzie, J. R. Cooper, Y. Maeno, S. Nishizaki, and T. Fujita, *Phys. Rev. B* **57**, 5505 (1998).
- [37] C. Bergemann, A. P. Mackenzie, S. R. Julian, E. Ohmichi, and N. Haugh, *Adv. Phys.* **52**, 639 (2003).
- [38] N. Kikugawa, C. Bergemann, A. P. Mackenzie, and Y. Maeno, *Phys. Rev. B* **70**, 134520 (2004).
- [39] Y. Krockenberger, M. Uchida, K. S. Takahashi, M. Nakamura, M. Kawasaki, and Y. Tokura, *Appl. Phys. Lett.* **97**, 082502 (2010).
- [40] C. Bergemann, S. R. Julian, A. P. Mackenzie, S. NishiZaki, and Y. Maeno, *Phys. Rev. Lett.* **84**, 2662 (2000).
- [41] K. M. Shen, N. Kikugawa, C. Bergemann, L. Balicas, F. Baumberger, W. Meevasana, N. J. C. Ingle, Y. Maeno, Z.-X. Shen, and A. P. Mackenzie, *Phys. Rev. Lett.* **99**, 187001 (2007).
- [42] J. Mravlje, M. Aichhorn, T. Miyake, K. Haule, G. Kotliar, and A. Georges, *Phys. Rev. Lett.* **106**, 096401 (2011).
- [43] L. de Medici, J. Mravlje, and A. Georges, *Phys. Rev. Lett.* **107**, 256401 (2011).
- [44] Y.-T. Hsu, W. Cho, B. Burganov, C. Adamo, A. F. Rebola, K. M. Shen, D. G. Schlom, C. J. Fennie, and E.-A. Kim, [arXiv:1604.06661](https://arxiv.org/abs/1604.06661).